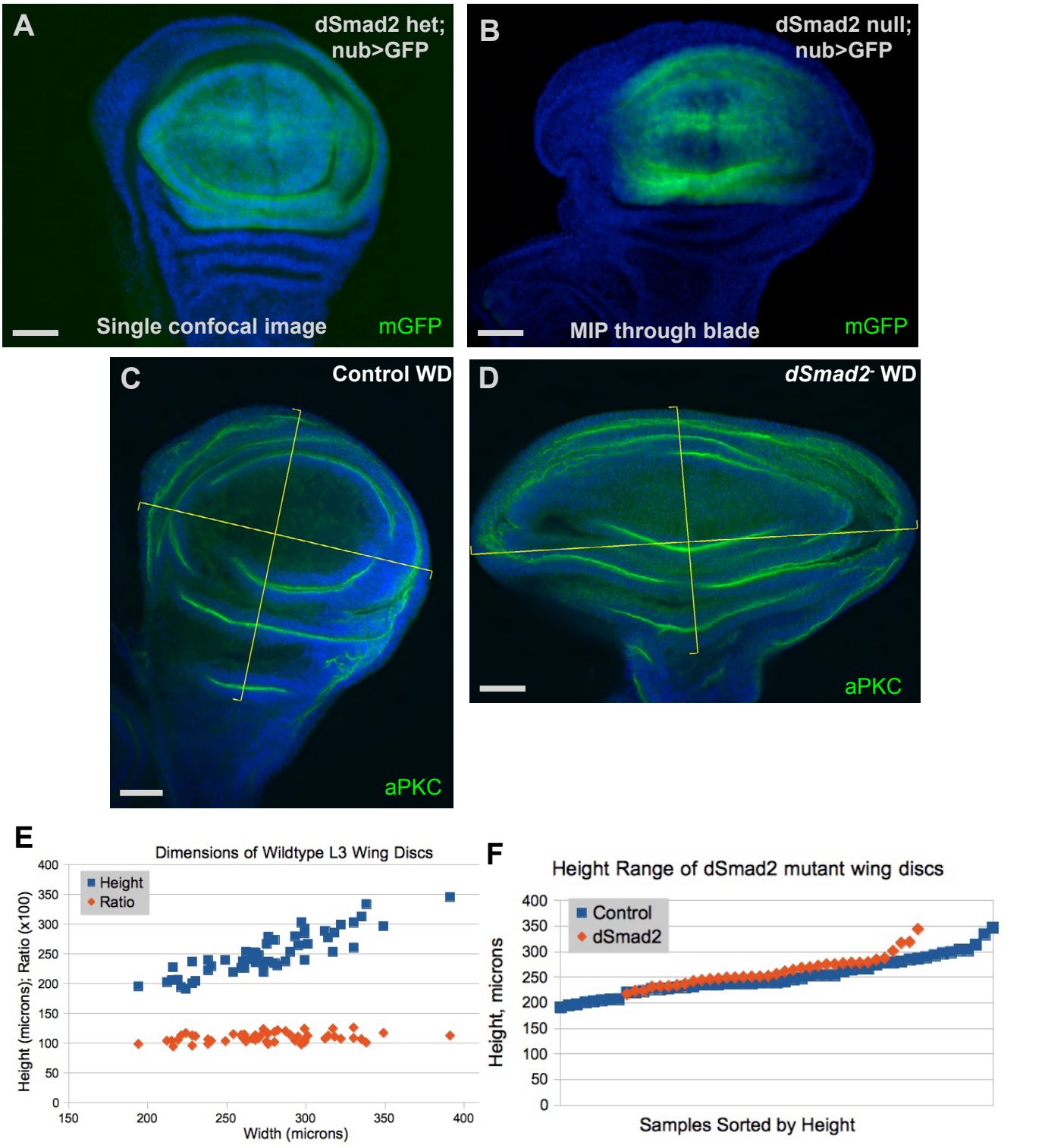

Fig. S1. Measuring wing disc ratio to track lateral overgrowth. (**A**,**B**) *nub*-GAL4 expression marking the pouch was monitored by a GFP reporter in control and *Smad2* null discs. Expression domain normally has sharp boundaries (A) but fades laterally in the *Smad2* mutant (B). (**C**,**D**) Wing disc dimensions were determined at stereotyped positions and used to calculate W/H ratio. Fixed discs were stained for DAPI to visualize nuclei (blue) and aPKC to mark epithelial folds (green). The notum primordium was excluded because it not does widen in the mutants. In these examples, the control ratio is 1.02 and the Smad2 mutant is 1.81. (**E**) The W/H ratio is nearly constant during L3 wing disc growth. Height (blue) plotted in relation to width shows a steady increase for normal wing discs. The W/H ratio for the same set of discs is plotted (orange, multiplied by 100 for visualization) to show that any change over time is minor compared with W/H ratio changes observed for *Smad2* loss-of-function wing discs. The variation in the measured values for a given genotype might derive from physical distortions introduced during dissection, fixation and mounting and/or might reflect true biological variation. (**F**) The range of measured wing disc heights is similar between control and *Smad2* mutant wing discs. The measured height values were sorted for each condition and plotted with the median for each set positioned at the center of the *x*-axis. Because the height does not change, the change in W/H ratio is caused by width changes in *Smad2* mutant discs. Scale bars: 50 μm.

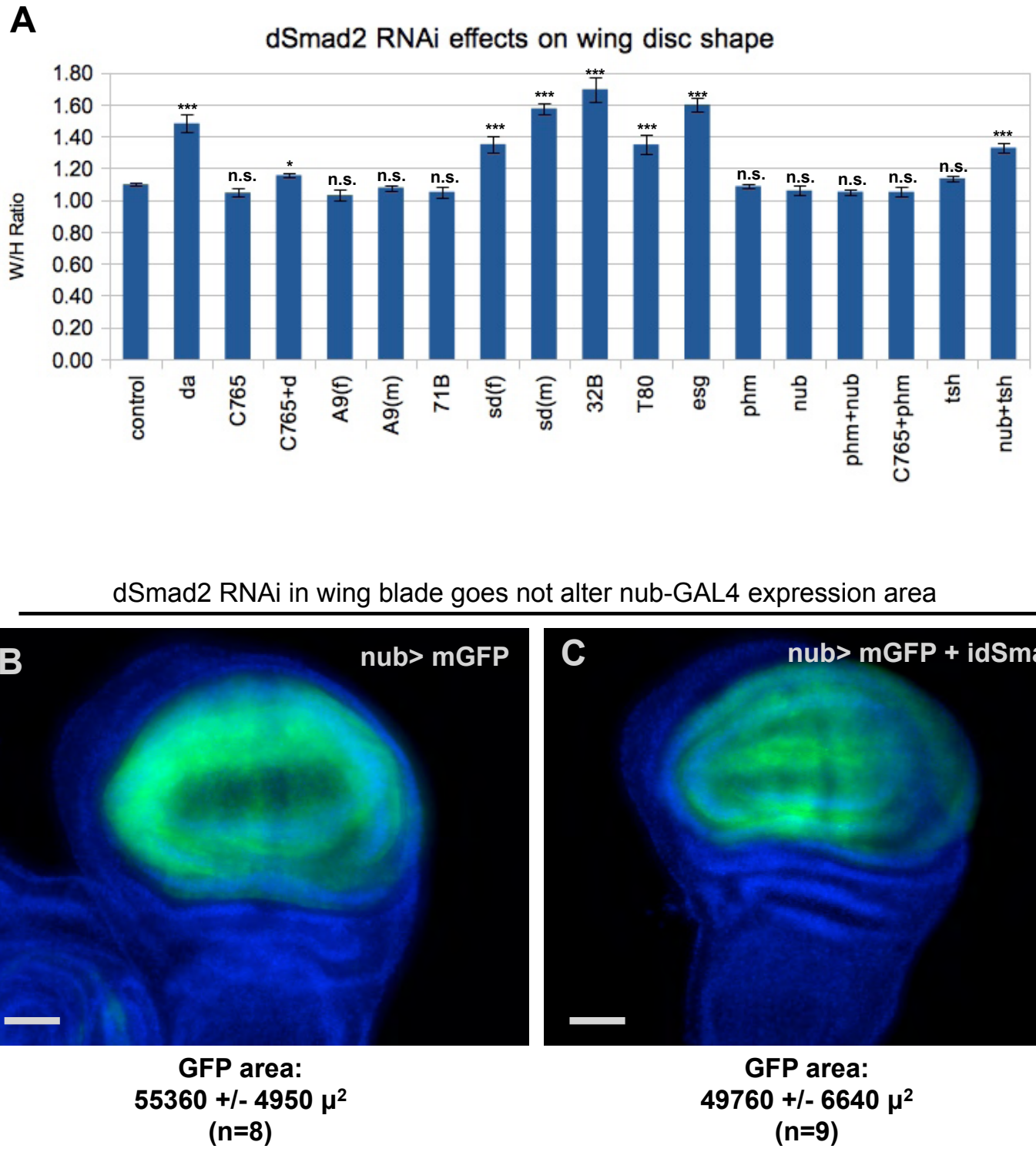

Fig. S2. Expanded results for dSmad2 RNAi effects on wing disc widening. (**A**) Summary of *Smad2* RNAi effects on wing shape for various GAL4 drivers. Control consists of a collection of wild-type and GAL4>GFP wing discs. For the remaining columns, the GAL4 driver or combination is listed. d is dicer-2. (f) and (m) indicate gender of the analyzed larvae. For each condition, the mean W/H ratio is plotted with s.e.m. as error bars. Statistical significance of one-tailed *t*-test is indicated. n.s., not significant. **P*<0.05; ****P*<0.001. (**B**,**C**) nub-GAL4 activity domain is unaffected by *nub>Smad2* RNAi. Width and height of the GFP-positive domain were measured from maximal intensity projections, and the area estimated by treating the area as an oval.

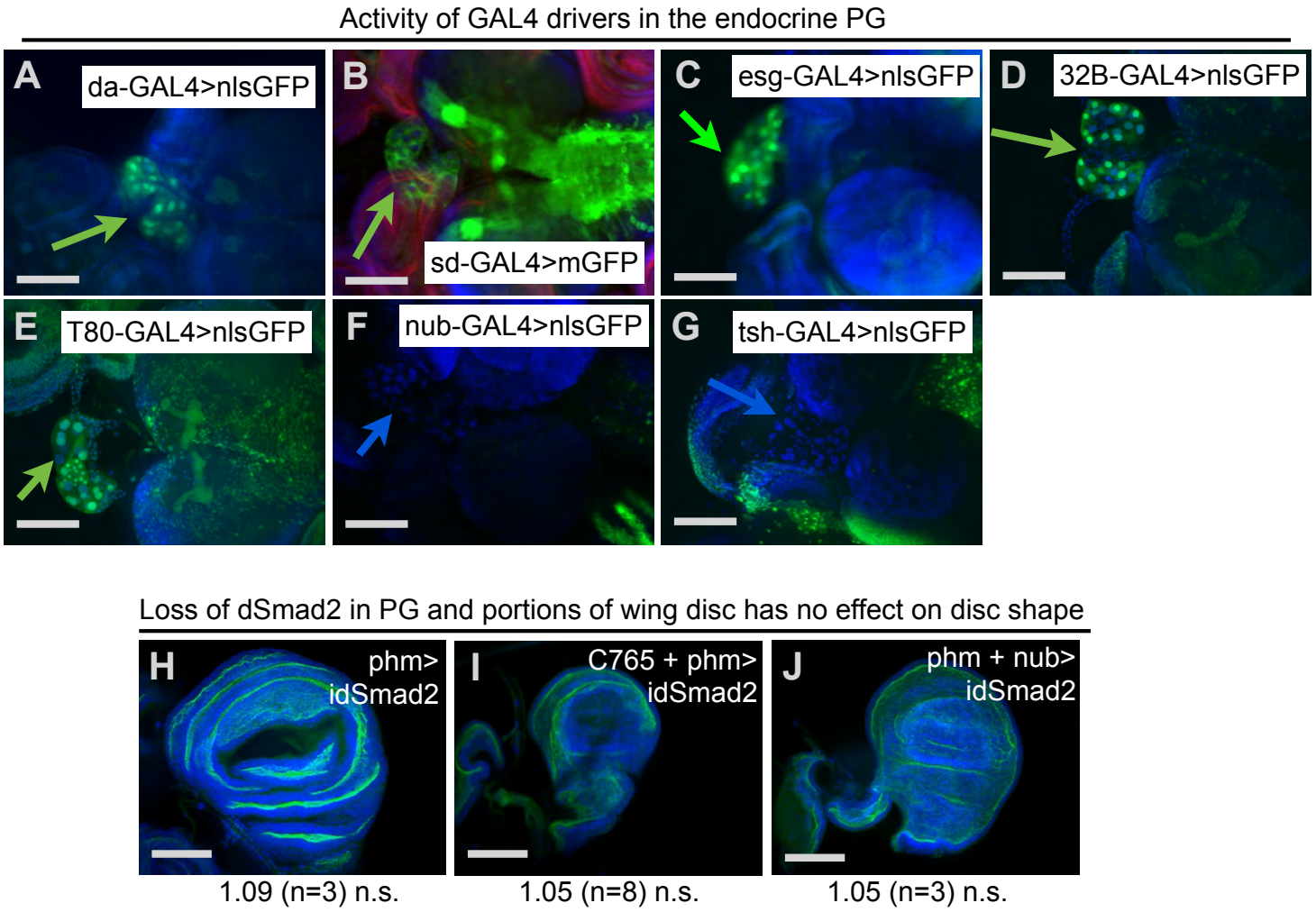

Fig. S3. GAL4 activity in the PG is unrelated to wing disc widening. (**A-G**) GAL4 activity in the prothoracic gland (PG). Many GAL4 drivers express in the PG, as revealed by UAS reporter analysis. All of the GAL4 drivers that individually caused wing disc widening with RNAi for *Smad2* are also active in the PG. *nub*-GAL4 and *tsh*-GAL4 are not active in the PG, but can cause disc widening when used in combination for Smad2 knockdown. GFP reporter is shown in green for all panels and green arrows point to reporter expression in the PG. Blue arrows in F and G point to the large nuclei of the PG cells that are negative for GFP. nlsGFP localizes to nuclei and mGFP is membrane bound. (**H-J**) Single driver *Smad2* RNAi using PG-specific *phm*-GAL4 did not lead to disc widening, nor did additive expression with C765 (I) or *nub* (J) wing disc GAL4 drivers. Data summarized as in Fig. 2. Scale bars: 50 μm.

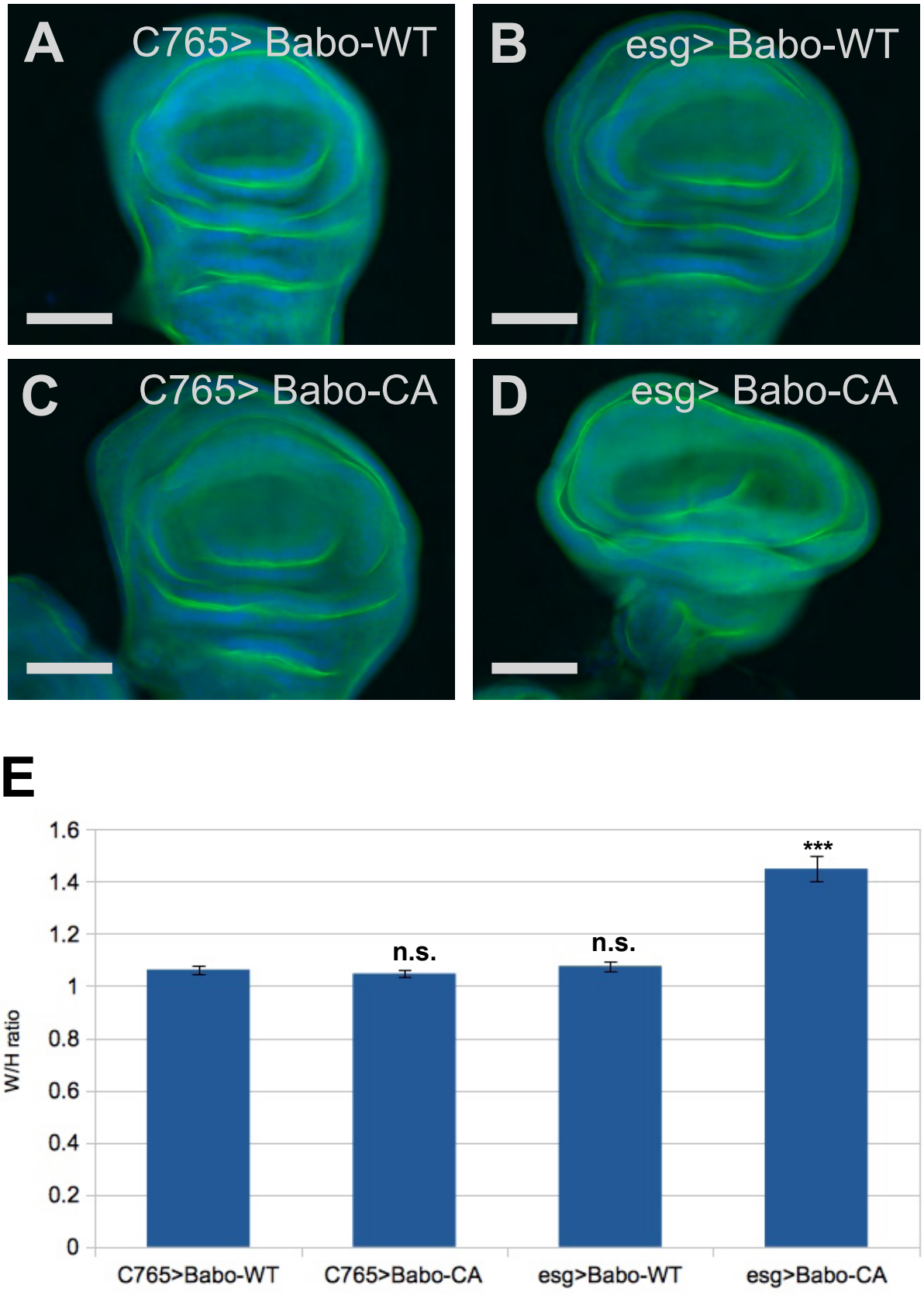

Fig. S4. Constitutively active Baboon can cause disc widening. (**A-D**) Fixed late L3 wing discs stained with DAPI (blue) and aPKC (green). Babo-WT or Babo-CA were expressed with the indicated drivers. (**E**) W/H ratio summary. ***P<0.001. n.s., not significant.

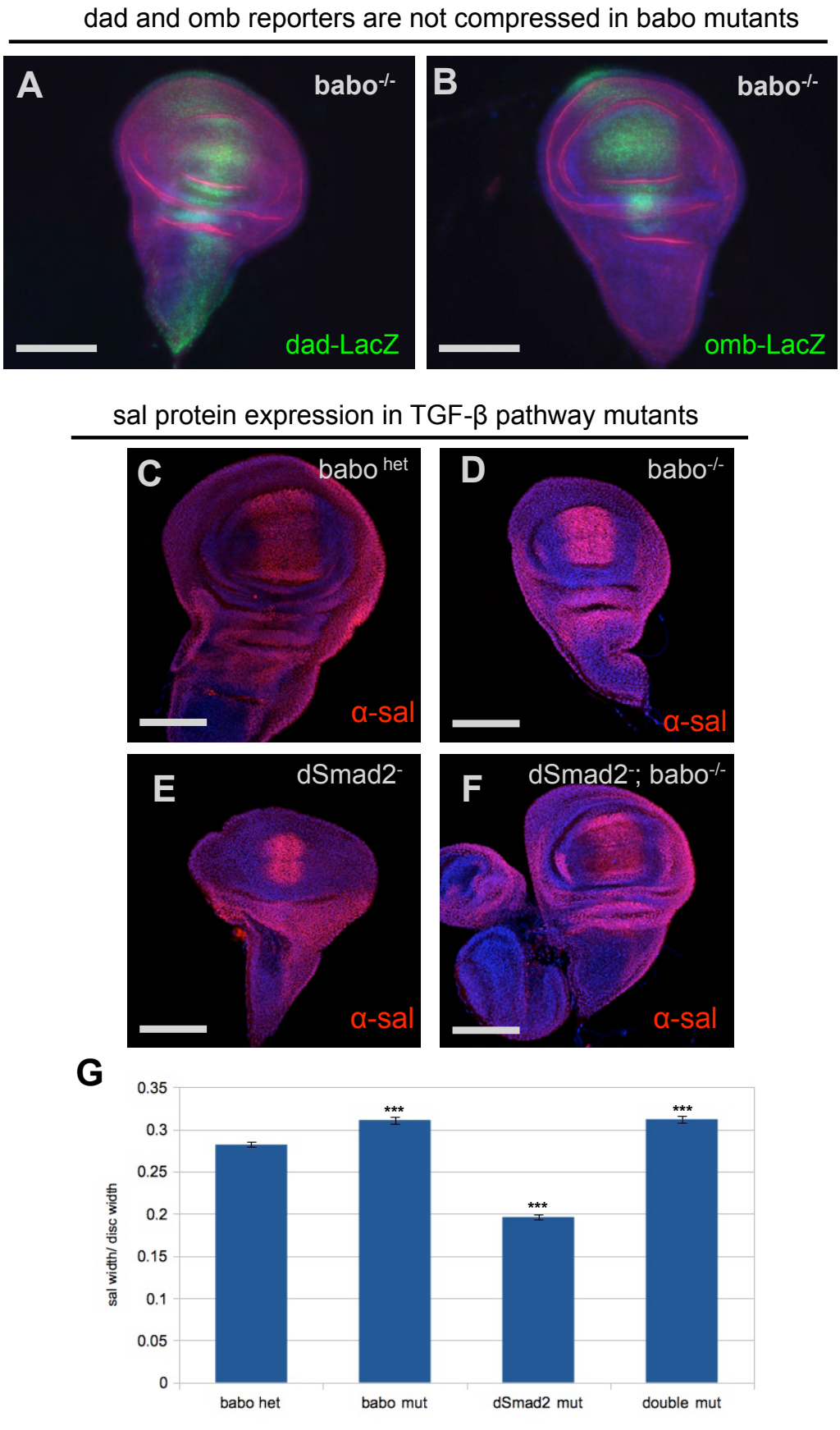

Fig. S5. Compression of dpp target gene expression is only seen in *dSmad2* mutants. (**A**,**B**) *Dad-lacZ* and *omb-lacZ* reporter expression in *babo* mutant discs showed nearly normal expression around the A/P axis. This contrasts with the narrowing or lack of scaling seen for Smad2 mutants (Fig. 5). (**C-F**) Endogenous Sal protein expression was assayed in a panel of genotypes. The Sal domain in the wing pouch occupied a slightly larger portion of the discs in *babo* mutants (D) and a much smaller portion in *Smad2* mutants (E), and the double mutant pattern resembled the *babo* pattern. (**G**) Results for Sal staining. ***P<0.001.

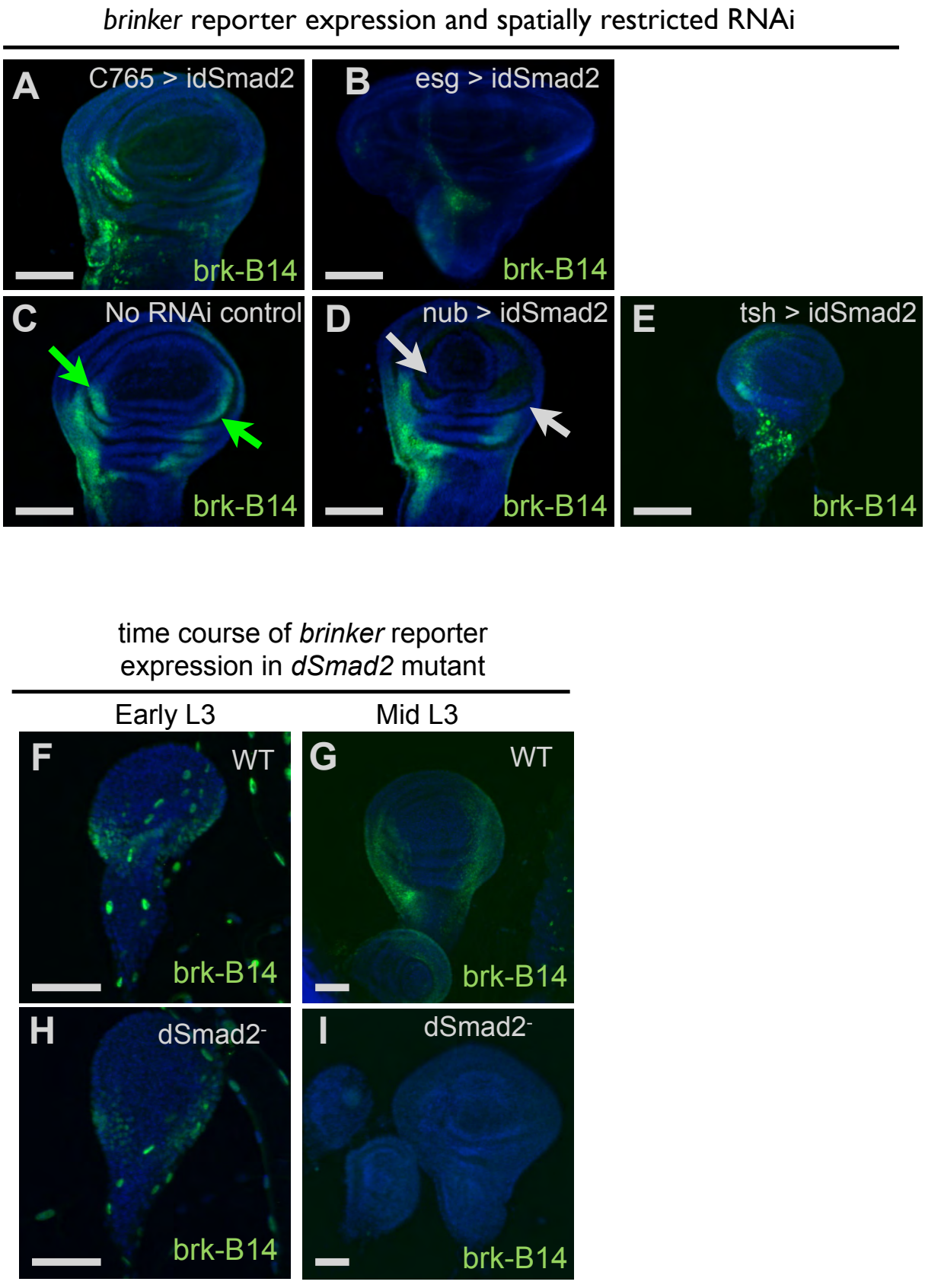

Fig. S6. Smad2 loss and *brinker* expression. (**A-E**) B14 expression loss correlates with wing disc widening. C765-Gal4 did not produce widening and patchy B14 expression remained in late L3 discs (A). *esg*-GAL4, which is active throughout larval development, caused widening and loss of B14 expression in the pouch and hinge disc regions (B). *Nub* and *tsh* GAL4 did not produce widening, and there was significant B14 expression (D,E). Portions of the B14 expression domain lost in *nub>idSmad2* are shown by arrows in C,D. Disc in E is undersized because *tsh-GAL4>idSmad2 + dicer* animals are sick and do not reach full size. Scale bars: 100 μm. (**F-I**) B14 expression time-course in *Smad2* mutants. Scale bars: 50 μm. Lateral B14 expression initiated normally in *Smad2* mutants (H versus F), but was lost by mid-L3 (I versus G). Imaging and display conditions identical for F,H and G,I. Large punctate green signals in F,H are tracheal cells.

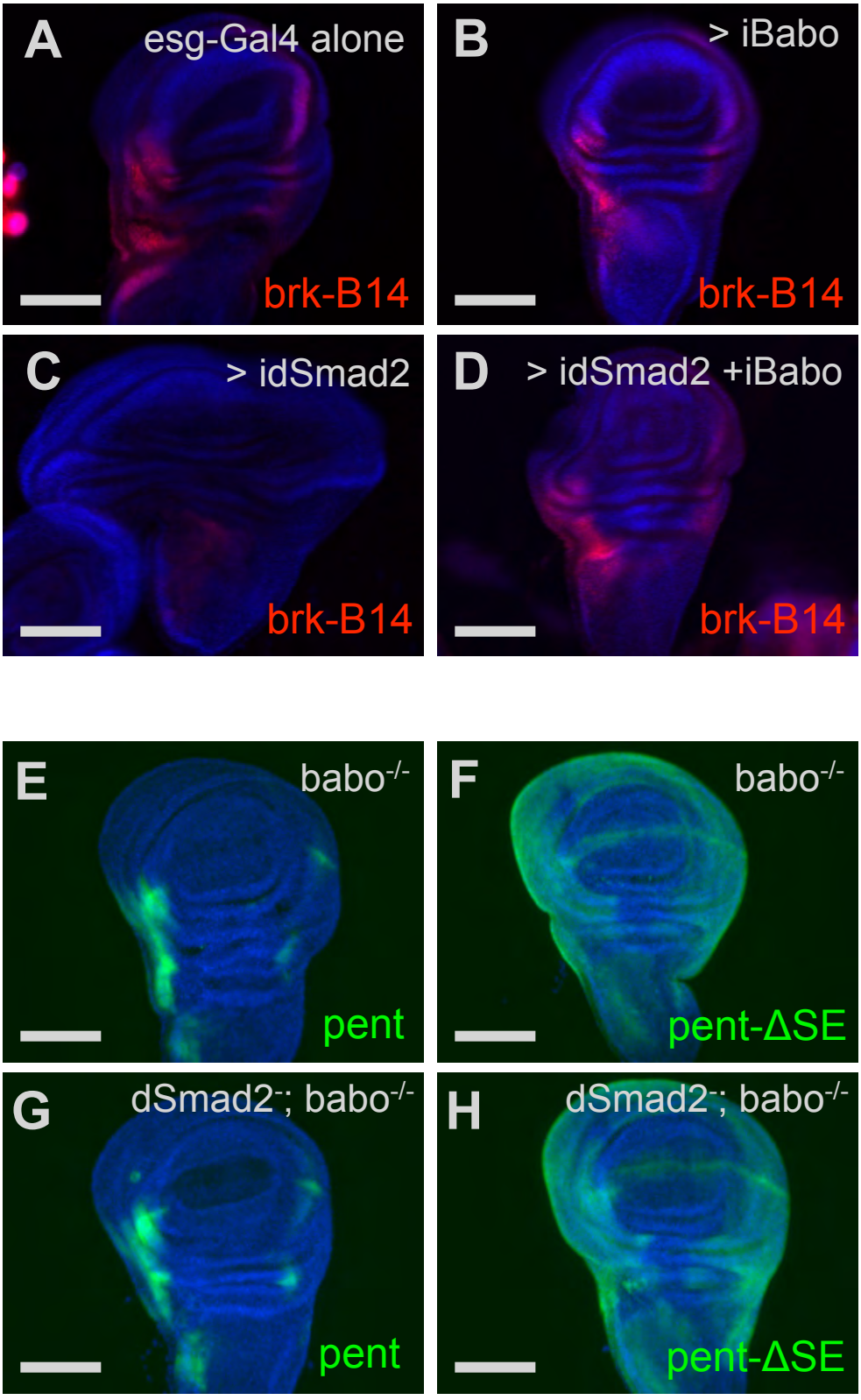

Fig. S7. Ectopic repression through the SE requires Baboon. (**A-D**) B14 expression under esg-GAL4>RNAi conditions that mimic epistasis test for Smad2 and Baboon. Loss of B14 expression is only seen with *idSmad2* (C). It is restored by simultaneous knockdown of Babo (D). (**E-H**) *pent* reporters are not affected by loss of baboon. Single *babo* mutant discs and *dSmad2; babo* double mutants have pent (E,G) and pent-ΔSE (F,H) expression in that same patterns as control discs (Fig. 6). Scale bars: 50 μm.

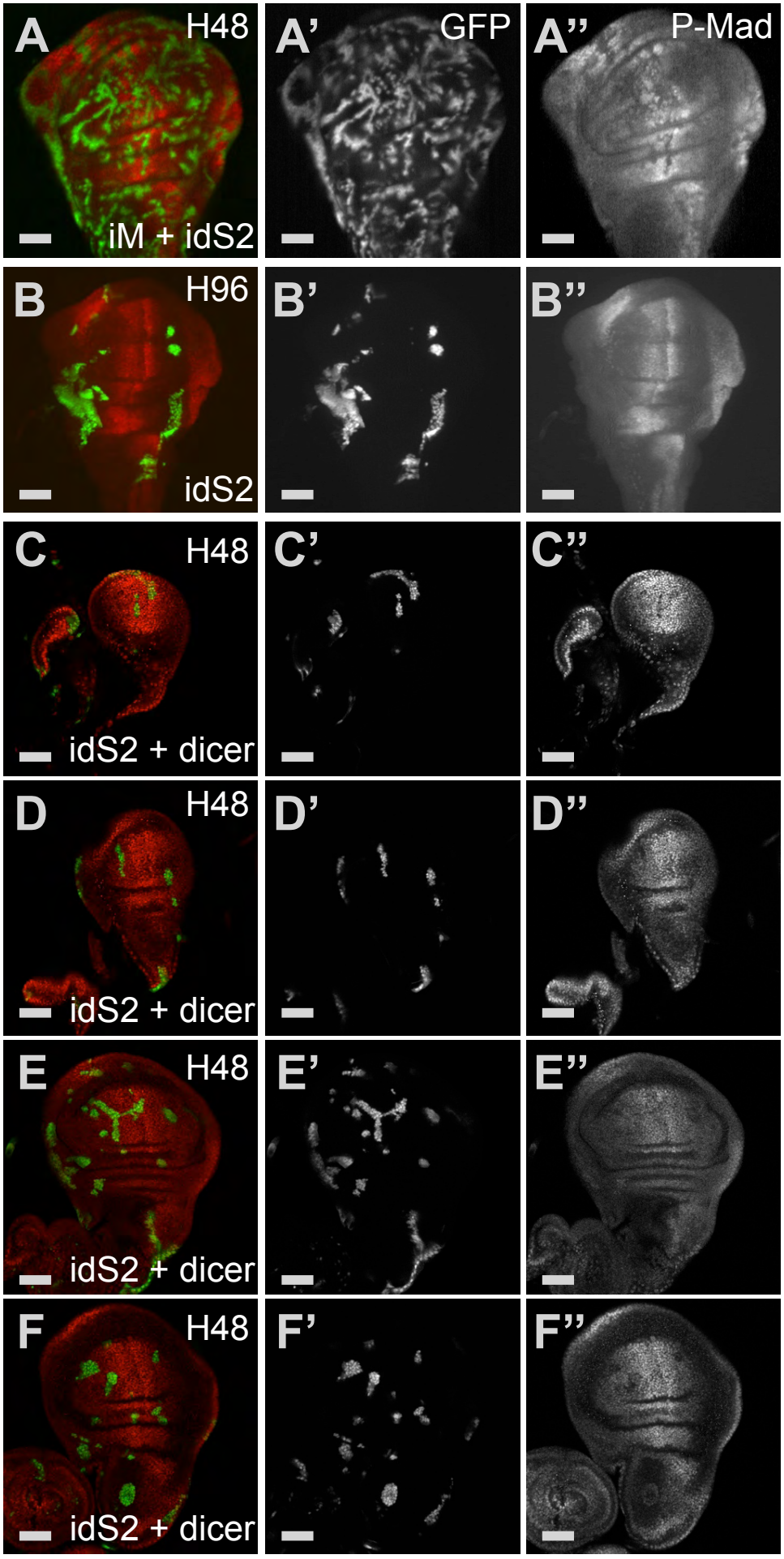

Fig. S8. Smad2 knockdown clones at different time points do not show increased P-Mad. (**A-F**) Immunohistochemical detection of P-Mad in flp-out RNAi clones under various conditions. For all panels, the two-color image shows GFP-marked clones in green and P-Mad staining in red. Single and double prime images are isolated GFP and P-Mad channels, respectively. (A) Mad and Smad2 RNAi knockdown clones are shown as a positive control for ability to detect P-Mad changes in wing disc clones 48 hours after clone induction (H48). (B) *Smad2* RNAi clones analyzed 96 hours after induction (H96) did not have increased P-Mad. Early L3 (C,D) and mid L3 (E,F) *Smad2* RNAi clones with dicer-2 co-expression often showed a decrease in P-Mad staining. A and B are maximal intensity projections, and C-F are single confocal sections. Scale bars: 50 μm.